East European Journal of Physics. 3. 74-84 (2025)
DOI:10.26565/2312-4334-2025-3-07 ISSN 2312-4334

MODELING OF THE CHARACTERISTICS OF ELECTRON BEAMS AND GENERATED PHOTON FLUXES ON THE M-30 MICROTRON

Eugene V. Oleinikov[a]*, David Chvátil[b], Eugene Yu. Remeta[a], Aleksandr I. Gomonai[a], Yurii Yu. Bilak[c]

[a]*Institute of Electron Physics, National Academy of Sciences of Ukraine, Uzhhorod, Ukraine*
[b]*Nuclear Physics Institute, Czech Academy of Sciences, Czech Republic*
[c]*Uzhhorod National University, Uzhhorod, Ukraine*
**Corresponding Author e-mail: zheka.net.ua@gmail.com*
Received May 6, 2025; revised July 10, 2025; accepted July 17, 2025

Ensuring optimization of the radiation treatment process of experimental samples at electron accelerators and effective prediction of the results of the interaction of electron beams with irradiation objects requires the most accurate information about the characteristics of the beams. The initial (primary) characteristics of accelerator electron beams during transportation to irradiation objects will change due to their interaction with the external environment (air). Thus, secondary particles are also generated - bremsstrahlung photons, which also interact with samples. The paper presents the results of studies on modeling the influence of air layers on the change in the initial characteristics of electron beams during their transportation to irradiation objects and on the parameters of the generated bremsstrahlung photon fluxes in the plane of placement of experimental samples. The studies used the Monte Carlo code – GEANT4. The modeling was carried out for the electron accelerator of the IEP NAS of Ukraine - the M-30 microtron, taking into account its technical parameters. The results of studies of the characteristics (energy spectrum, their integral values, transverse distributions in the 10×10 cm plane) of the electron beam and secondary photons at the output of the electron accelerator are presented. The influence of the thicknesses of the air layers (0.1÷500 cm) between the electron output unit and the potential plane (100×100 cm) of the placement of experimental samples for irradiation on the characteristics of the primary electron beams and generated bremsstrahlung photons (for the energy range of 6÷20 MeV) is studied.
Keywords: *Microtron; GEANT4; Electron beam; Bremsstrahlung; Ti window; Air; Spectra; Spatial distributions*
PACS: 29.17.+w, 29.27._a

INTRODUCTION

Electron beams obtained from electron accelerators (linear, microtrons [1]) are used to solve both scientific [2] and a wide range of applied problems [3-9]. These problems are related to the improvement of radiation therapy protocols in the practice of treating oncological diseases [3]; to the protection of personnel during the operation of accelerators [4], sterilization of medical drugs and devices for their disinfection [5]; processing of food products to increase their shelf life [6]; creation of promising materials with predetermined technical parameters that are necessary for the development of modern innovative technologies [7], alternative methods of producing medical radioisotopes [8]; to non-destructive analysis of nuclear materials for the purpose of their control and non-proliferation [9] and many others. To solve these problems, it is necessary to have the most accurate information about the characteristics (energy spectra, their integral values, transverse distributions along the potential placement plane (PPP) of experimental samples [10,11]) of electron beams interacting with the irradiated objects. In this case, it is important to determine the factors that will influence these final characteristics of the beams during their transportation to the irradiated materials and interaction with them.

The initial (primary) characteristics of electron beams during transportation between the accelerator output unit and the irradiated sample PPP will change due to their interaction with the environment, usually air, due to the processes of inelastic collisions with atomic electrons and nuclei. These processes lead to ionization and excitation of atoms (ionization losses) and the formation of bremsstrahlung (radiation losses) [12]. That is, the initial energy of the beam electrons is lost (decreases) due to inelastic collisions - excitation, ionization, and the formation of bremsstrahlung photon fluxes. In elastic collisions, electrons' kinetic energy and momentum can be redistributed between particles [12]. We also note that secondary particles – photons and electrons – will be present in the electron beams, which are formed by the above processes during the transport of electrons in the layers of matter (air) [13,14].

To ensure the uniformity of the transverse distribution of electron beams along the PPP of the irradiation objects, the distance from the electron output blocks of the accelerators to them is increased, which leads to an increase in the thickness of the air layers and, accordingly, to an increase in the number of secondary photons [15-17]. Secondary photons will also be formed at the outputs of the electron output blocks (between vacuum and air) due to their interaction with the structural elements of the accelerators [18,19]. Reliable information about the characteristics of the secondary photon fluxes in electron beams and the relationships between them is necessary when planning and optimizing (observing the uniformity of the particle field in the PPP of the samples, taking into account their geometric dimensions) the process of irradiation of experimental samples on electron accelerators [15-17]. It should be noted that data on the characteristics of

Cite as: E.V. Oleinikov, D. Chvátil, E.Yu. Remeta, A.I. Gomonai, Yu.Yu. Bilak, East Eur. J. Phys. 3, 74 (2025), https://doi.org/10.26565/2312-4334-2025-3-07

secondary photon fluxes in electron beams are also used to develop methods for determining the characteristics (spectral, integral, and transverse distributions in the PPP of experimental samples) of electron beams when direct measurements are not possible [20,21].

Results of current research (both theoretical and experimental) into the process of transporting electron beams (with energies up to 20 MeV) from the accelerator output blocks to the irradiation objects indicate the influence of air layers (from 0.1 to 700 cm) on the specified final characteristics, as well as on the characteristics of the photon fluxes generated by them in the PPP of experimental samples [22,23]. With increasing distance to the irradiation objects, these characteristics of electron beams will change at fixed values of the initial electron energy [24,25]. Thus, electron energy's nominal values (in the PPP) will decrease relative to their initial values [24,25]. It should also be noted that the efficiency of generating bremsstrahlung photon fluxes by electron beams in the PPP will increase [26,27].

The final characteristics of electron beams and generated photon fluxes in the PPP are significantly influenced by the initial values of electron energies at fixed distances between the electron output units of the accelerators and the irradiation objects [26]. Thus, with an increase in beam energy (energy range 6÷20 MeV), electron scattering in air decreases [12,22], and the efficiency of secondary photon generation increases [12,15].

Analysis of the results of existing experimental and theoretical studies of the influence of air layers on the change in the final characteristics of electron beams and generated secondary photon fluxes in the PPP (under practically the same conditions of conducting experimental studies on electron accelerators with different technical parameters) indicates their dependence on the characteristics of the primary (initial) electron beams (their geometric dimensions, the shape of the spatial distributions at the accelerator output and energy) [28,29]. Any differences between the characteristics of primary electron beams on different types of accelerators depend on their technical parameters and design features of the output (electron) blocks, since they determine their initial characteristics [28,29].

Therefore, for the successful use of electron accelerators to ensure the experimental samples' irradiation process, reliable data on the characteristics of electron beams and secondary photon fluxes that interact with the irradiation objects are required for each type of accelerator. These data are necessary for optimizing the process of irradiation of experimental samples with electron beams - ensuring their uniformity in the PPP of experimental samples, obtaining the expected value of the absorbed dose (taking into account the energies, intensity, spatial and angular distributions of electron beams in the PPP, geometric dimensions of experimental samples), and reliable assessment of the contribution of the additional absorbed dose from the specified secondary, bremsstrahlung, photons.

The presented work aimed to study the influence of the initial parameters of electron beams (during their transportation to irradiation objects) and air layers on their final values and characteristics of the generated fluxes of secondary photons in the PPP of experimental samples.

The research was conducted using the electron accelerator of the Institute of Electron Physics of the National Academy of Sciences of Ukraine – the M-30 microtron. Its main technical parameters (design of the electron output unit, range of accelerated electron energies, average effective beam current) [30] are similar to those of most operating accelerators in our country [31].

MATERIALS AND METHODS

For computer calculations of the process of transporting electrons and the secondary photons generated by them in the titanium (Ti) window of the electron output unit of the M-30 microtron and the air layers between the output unit and the PPP of the irradiation materials, a program was developed based on the GEANT4 v11.1 toolkit [32]. The created program specified a list of physical processes FTFP_BERT_HP, which uses the physical model of electromagnetic interaction standard for GEANT4 [33,34]. The modeling took into account the design features of the electron output unit of the M-30 microtron [35,36] and the initial parameters of the electron beam that were defined in the DetectorConstruction and PrimaryGeneratorAction classes, respectively [3]. GEANT4 visualization methods based on the Win32 API were used to verify the irradiation scheme.

The simulations were performed for uncollimated electron beams with an equal probability distribution [22], which had the shape of an ellipse with axes of 22 and 6 mm [35,36]. The initial electron energy varied from 6 to 20 MeV. During the simulations, all electrons and the secondary photons, generated by them, that fell into planes perpendicular to the axis of the initial electron beam were recorded - 10×10 cm (at the accelerator output) and 100×100 cm (in the PPP of the materials for irradiation). Visualization of the results of modeling electron transport and secondary photon generation using the GEANT4 toolkit in the absence and presence of air layers is shown in Figure 1.

The modeling was carried out in two stages.

First stage: the characteristics (energy spectra, integral and transverse distribution) of electron beams and secondary photon fluxes generated in the Ti window and their content in the electron beam at 1 mm distance from the accelerator output unit in a 10×10 cm plane were studied.

The second stage is the study of the influence of air layers between the accelerator output unit and the PPP of the irradiation materials on the generation of secondary photon fluxes by the electron beam and their content in the beams that fell into the PPP of experimental samples (100×100 cm) at five fixed distances (100÷500 cm) from the output unit.

The simulated energy spectra of electrons and secondary photons falling into the PPP were normalized to one initial electron.

The integral values N of the number of electrons N_e and secondary photons N_γ were calculated according to formula (1) from the corresponding obtained energy spectra $\phi(E)$:

$$N = \int_0^{E_{max}} \phi(E) dE. \quad (1)$$

The percentage of secondary photons in the electron beam was determined by the formula

$$C = \frac{N_\gamma}{N_e} \cdot 100\%. \quad (2)$$

Based on the simulation results, probability heat maps of the transverse distribution of electron beams and secondary photon fluxes in the PPP were created using the ORIGIN package [7] for visualization.

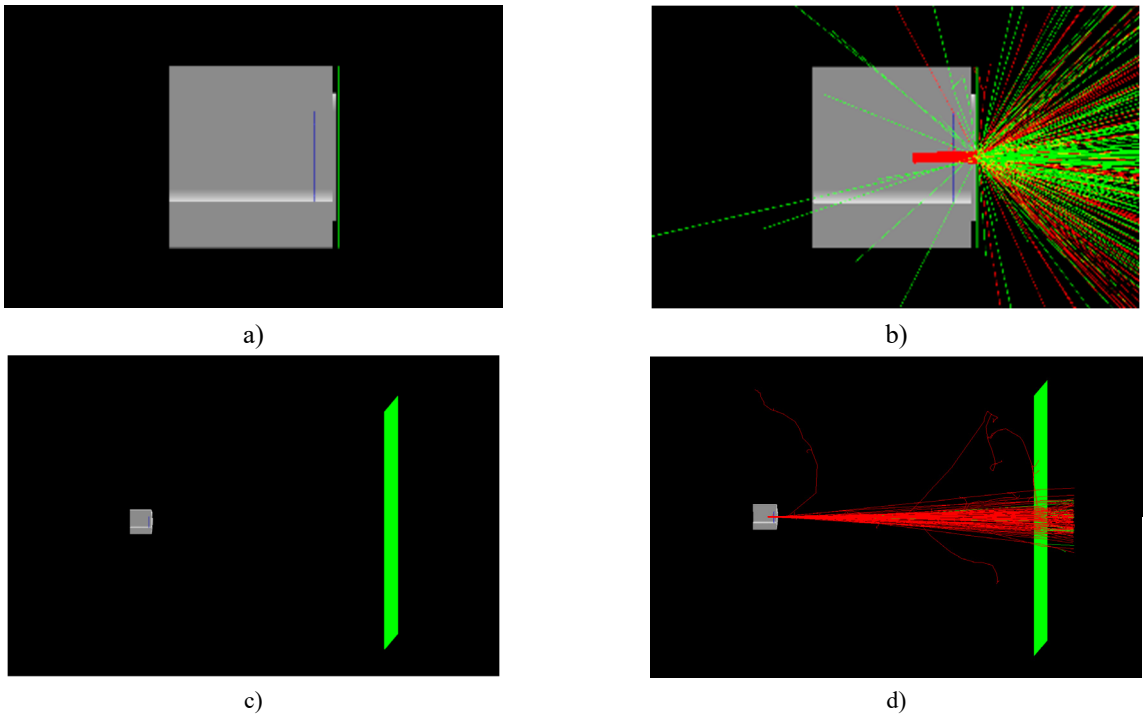

a) b) c) d)

Figure 1. Visualization of modeling results for Ti windows in the absence (a, b) and presence (c, d) of air layers using the GEANT4 toolkit (grey – electron output unit; green square - PPP; red and green lines – electron and photons path).

RESULTS AND DISCUSSION

As a result of the simulations conducted, the following were investigated:

- changes in the characteristics (energy spectra, their integral values, and transverse distributions in the PPP) of the initial electron beam and photon fluxes generated by electrons during interaction with the Ti window of the output unit of the M-30 microtron and their content in the electron beam in the plane of the output unit;
- changes in the characteristics of electron beams and photon fluxes generated by electrons during interaction with air layers between the plane of the output unit and the PPR of the irradiated objects, and the relative content of photon fluxes in electron beams.

Effect of titanium window on electron beam characteristics and secondary photon generation

As a result of the simulations, the characteristics of the energy spectra of electron beams (after their interaction with the Ti layer) and the fluxes of secondary photons (generated by the Ti layer) in the plane of the output unit of the M-30 microtron (10×10 cm), perpendicular to the electron beam axis (Figure 2), were calculated. The calculations were performed for initial electron energies from 6 to 20 MeV.

It is established that the numerical integral values of the number of electrons $N_{e/e}$ in the beam after their interaction with the Ti layer are practically constant for the specified energy range. In contrast, the numerical integral values of the number of photons $N_{\gamma/e}$ in the fluxes increase with increasing initial electron energy from 8.117×10^{-4} γ/e (at 6 MeV) to 0.00101 γ/e (at 20 MeV). Their percentage content in electron beams C also increases slightly from 0.08061% to 0.1003% with increasing initial electron energy from 6 MeV to 20 MeV.

From the simulation results, the profiles of electron beams and bremsstrahlung photons on a plane measuring 10×10 cm at the accelerator output were obtained (Figure 3). From the obtained profiles, the transverse distribution of the intensity of electrons and secondary photons along the X axis perpendicular to the beam axis in the plane's center was taken (Figure 4). An increase in the energy of the initial electron beam from 6 MeV to 20 MeV does not affect the transverse distribution of the electron beam in the plane at the accelerator output (the numerical value is ~6.1547×10^5),

whereas in the case of bremsstrahlung photon fluxes, their integral number increases by ~1.5 times (from ~419.3 to ~605.4), but this increase is not significant.

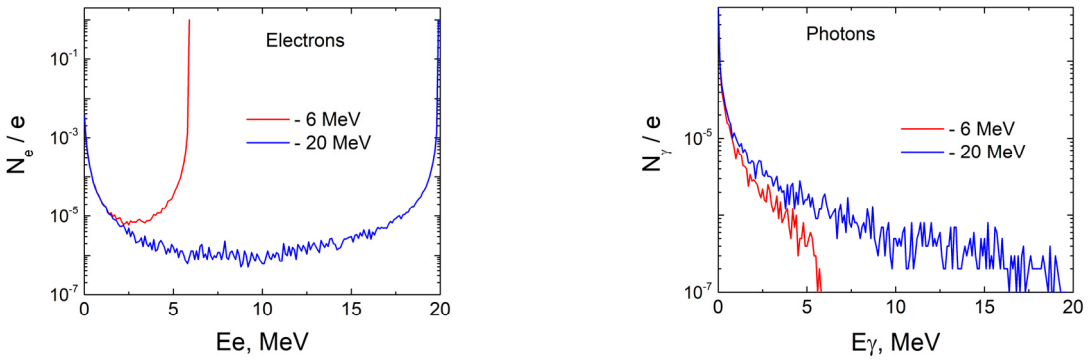

a) b)

Figure 2. Dependence of the energy spectra of electron beams (a) and generated fluxes of secondary photons (b) on the initial energy of electrons after their interaction with the Ti layer.

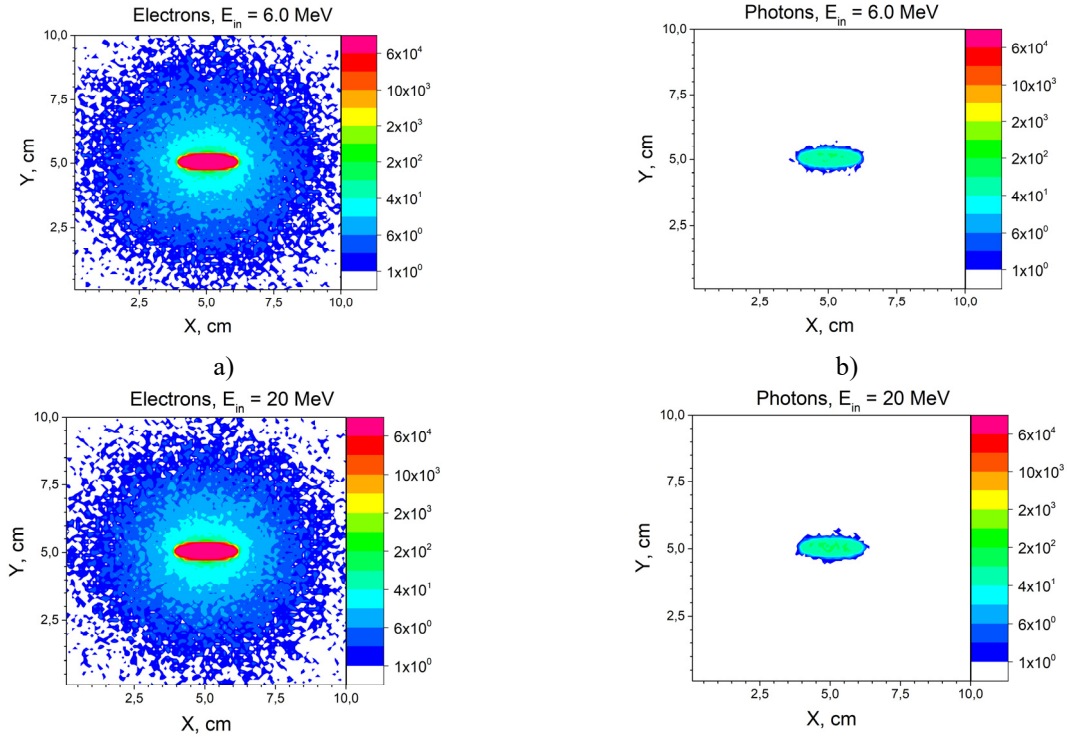

a) b)

c) d)

Figure 3. Profiles of electron beams (a, c) and secondary photon fluxes (b, d) at fixed values of initial electron energies of 6 MeV (a, b) and 20 MeV (c, d).

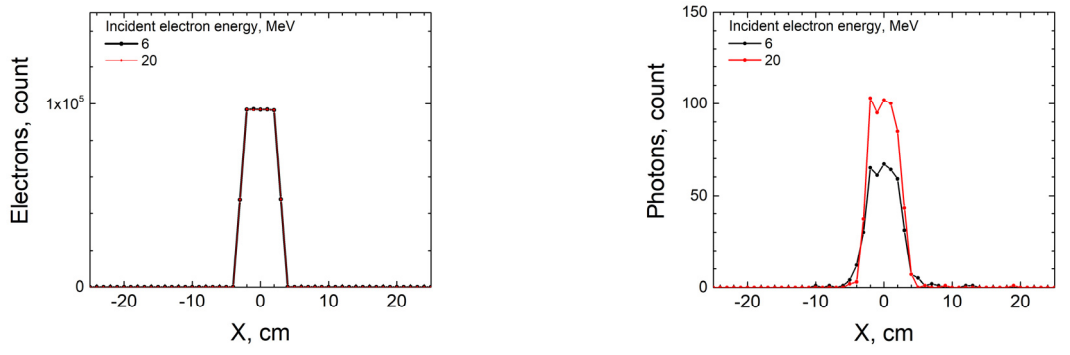

a) b)

Figure 4. Transverse distributions of electron beams (a) and secondary photon fluxes (b) at fixed values of initial electron energies of 6.0 and 20.0 MeV.

The calculations reflect the general patterns of the characteristics of the electron beams at the output in different models of accelerators, where Ti plates are used for the electron extraction schemes from vacuum to air [18,19]. The same applies to the fluxes of secondary photons generated by electrons in Ti windows. Possible differences in the results may be associated with the difference in technical parameters (design features of the electron extraction units, geometric dimensions) and with the initial electron energies used.

The influence of air layers on the characteristics of the initial electron beams and the generation of secondary photons

The implemented modeling allowed us to investigate the influence of air layers located between the electron output unit of the accelerator - the M-30 microtron and the PPP of experimental samples on the change in the initial characteristics of electron beams during their transportation to the irradiation object and the generation of secondary photons by them. The dependences of the final characteristics of electron beams in the PPP and the fluxes of secondary photons in the air on the initial energies of the electrons were established.

Calculations of the parameters (energy spectra, their integral values, transverse particle distributions in the SPP) of electron beams and the secondary photons generated by them in the PPP of the irradiated objects were carried out for a wide range of initial electron energies - 6÷20 MeV and distances between the output unit and the PPP - 0.1÷500 cm. The established parameters of the initial electron beam at the output of the output unit of the M-30 microtron, which took into account its technical characteristics, were used as input data when conducting simulations.

The results of simulations of the energy spectra of electron beams entering the PPP, depending on their initial energies (E_{in} = 6, 8, 10, 12.5, 14.5, 17.5, and 20 MeV) at fixed values of the distance – 100, 300 and 500 cm, and similar dependencies for the generated fluxes of secondary photons are presented in panel Figure 5. The energy spectra of electron beams and generated secondary photons fluxes in the PPP, depending on the distance (0.1, 100, 200, 300, 400, and 500 cm) at fixed values of the initial electron energy of 6.0, 12.5, and 20.0 MeV, are presented in panel Figure 6.

The simulation results (see Figures 5 and 6) indicate the dependence of the final spectral characteristics of electron beams in the PPP of irradiated objects on the thicknesses of the air layers (between the electron output unit and the PPP) through which they are transported and on their initial energies.

Analysis of the obtained results indicates a decrease in the numerical values of the nominal energy of electron beams in the PPP of experimental samples with an increase in the distance from 0.1 cm to 500 cm. The dependence of the nominal energy of electrons on the distance at fixed values of their initial energy is presented in Table 1.

Calculations were performed using our program to compare the obtained data with the results of similar studies (with the same initial electron energies and distances between the electron output blocks and the PPP of the irradiation objects) [38-40]. The results of the calculations of the energy dependences of the deviations of the nominal values of electron energies from their initial values are presented in Figure 7. The obtained results are consistent with each other. The deviations are associated with the experimental uncertainty of the literature data [38-40].

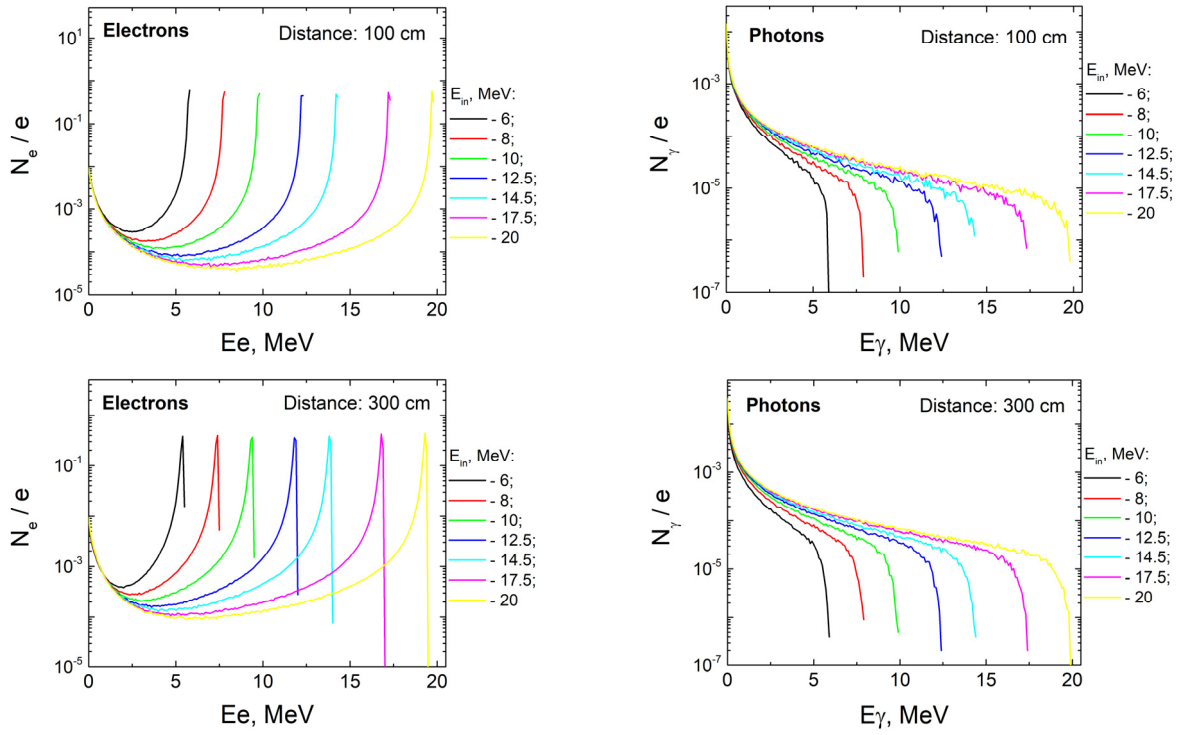

Figure 5. Energy spectra of electron beams and secondary photon fluxes in the PPP depending on the initial electron energy and fixed distance values – 100, 300, and 500 cm

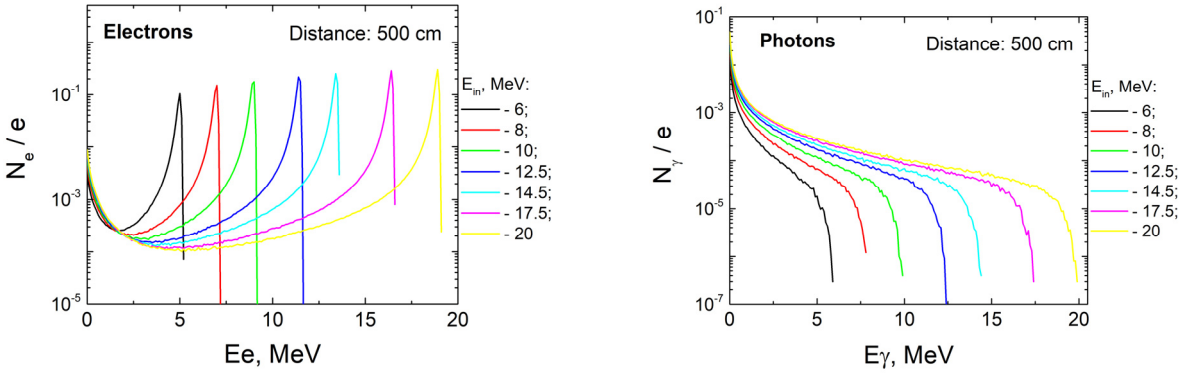

Figure 5. Energy spectra of electron beams and secondary photon fluxes in the PPP depending on the initial electron energy and fixed distance values – 100, 300, and 500 cm *(continued)*

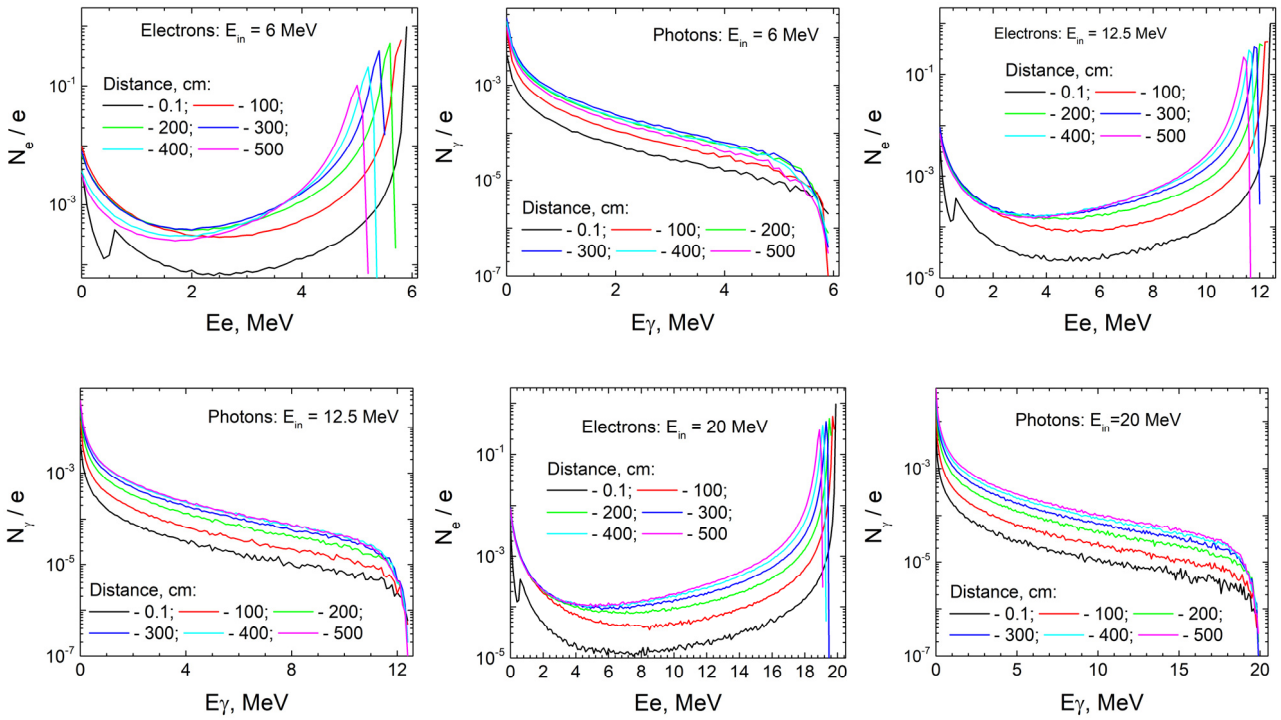

Figure 6. Energy spectra of electron beams and secondary photon fluxes depending on the distance at fixed values of initial electron energies – 6, 12.5, and 20 MeV

Table 1. Nominal value of electron beam energy in the PPP of experimental samples

Initial electron energy, MeV	Nominal energy change interval at distances 0.1–500 cm, MeV	Distances (cm)					
		0.1	100	200	300	400	500
		Nominal energy (MeV)					
6.0	~6.0 ÷ ~5.2	~ 5.9	~ 5.8	~ 5.7	~ 5.5	~ 5.3	~ 5.2
8.0	~8.0 ÷ ~7.2	~ 7.9	~ 7.8	~ 7.7	~ 7.5	~ 7.3	~ 7.2
10.0	~10.0 ÷ ~9.2	~ 9.9	~ 9.8	~ 9.7	~ 9.5	~ 9.3	~ 9.2
12.5	~12.5 ÷ ~11.6	~ 12.4	~ 12.3	~12.1	~ 12	~ 11.8	~ 11.6
14.5	~14.5 ÷ ~13.6	~ 14.4	~ 14.3	~14.1	~14.0	~13.8	~13.6
17.5	~17.5 ÷ ~16.6	~ 17.4	~ 17.3	~17.1	~16.9	~16.8	~16.6
20.0	~20 ÷ ~19.1	~ 19.9	~ 19.8	~19.6	~1 9.5	~19.3	~19.1

The obtained energy spectra of electron beams and secondary photon fluxes were used to calculate their integral values according to (1) and the percentage of secondary photons in the electron beam according to (2). Figure 8 shows the dependences of the integral quantitative values of electron beams and secondary photon fluxes on the initial electron energies (6 ÷ 20 MeV) at fixed distances 0.1÷500 cm, and the percentage of secondary photons in the electron beams.

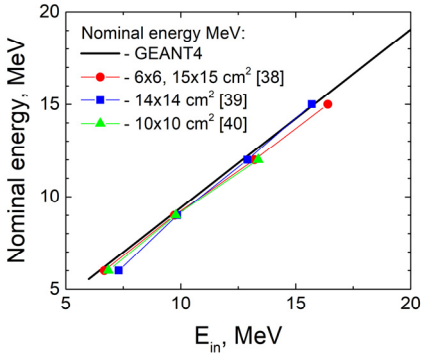

Figure 7. Dependence of the nominal values of electron energies on their initial values for different detection planes.

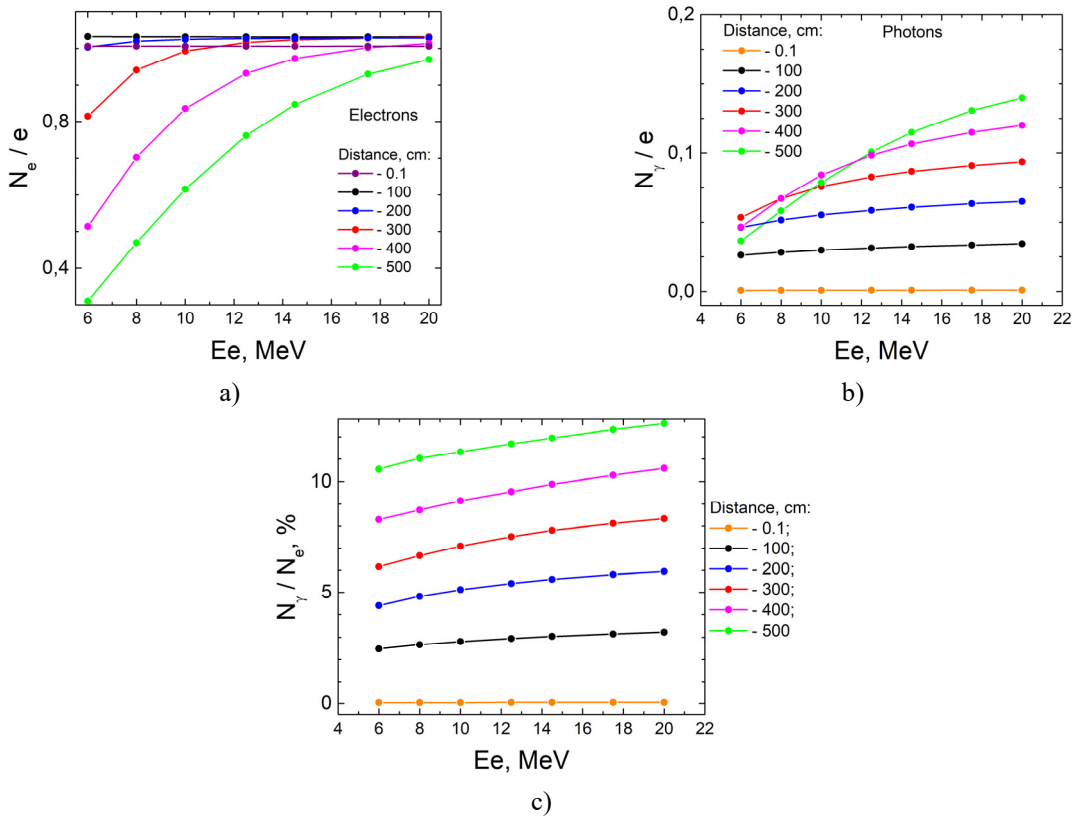

Figure 8. Dependence of the integral values of the quantities of electrons (a) and secondary photons (b), and the percentage of photons in the electron beam (c), on the initial energy of electrons at fixed distances

Similar dependences of the integral values of electron beams and secondary photon fluxes on the distances (0.1÷500 cm) at fixed initial electron energies 6÷20 MeV and the percentage of secondary photons in the electron beams are presented in Figure 9.

The dependence of integral quantitative values of electrons and secondary photons, falling on the PPP, on the energy at fixed distances and the percentage of secondary photons in the electron beam are given in Table 2.

Analysis of the calculated integral values of the electron beam N_e/e indicates their significant dependence on the thickness of the air layers through which the beam is transported and on its initial energy (Figure 8a, Figure 9a, Table 2). The integral values decrease at fixed initial electron energies with increasing distance to the irradiation objects. The initial energy of the beam at fixed distances significantly affects the rate of decrease of N_e/e. Thus, at a fixed initial energy of 6 MeV, the numerical values N_e/e decrease from 1.0060 to 0.3099 with a change in distance from 0.1 cm to 500 cm. And at a fixed initial energy of 20 MeV, the numerical values of N_e/e decrease slightly from 1.0060 to 0.9699 (with a similar change in distances from 0.1 cm to 500 cm).

The integral values of the bremsstrahlung photon fluxes N_γ/e generated by electron beams in the air layers between the output unit and the PPP of the experimental samples are determined by the thicknesses of the layers and the initial energies of the electrons (Figure 8b, Figure 9b, Table 2). The rate of change of N_γ/e is significantly affected by both the initial energy of the electrons and the distances. At a fixed initial energy of 6 MeV, the value of N_γ/e changes significantly from 8.117×10^{-4} to 0.0366, with a change in distances from 0.1 cm to 500 cm. And at a fixed initial energy of 20 MeV, the numerical values of N_γ/e change significantly from 0.0010 to 0.1399 with a similar change in distances from 0.1 cm to 500 cm.

With the increase in the initial electron energy and the increase in the distance, the probability of generating bremsstrahlung photons in the PPP of experimental samples increases. Therefore, the percentage content *C* (see (2)) of bremsstrahlung photon fluxes in electron beams increases (Figure 8c, Figure 9c, Table 2). It should be noted that the distance factor plays a key role here. With an increase in the distance from 0.1 cm to 500 cm, the numerical values of *C* increase from 0.04% to 10.55% at a fixed initial electron energy of 6 MeV. Almost similar changes occur at a fixed electron energy of 20 MeV. Here, the numerical values of *C* increase from 0.05% to 12.60%.

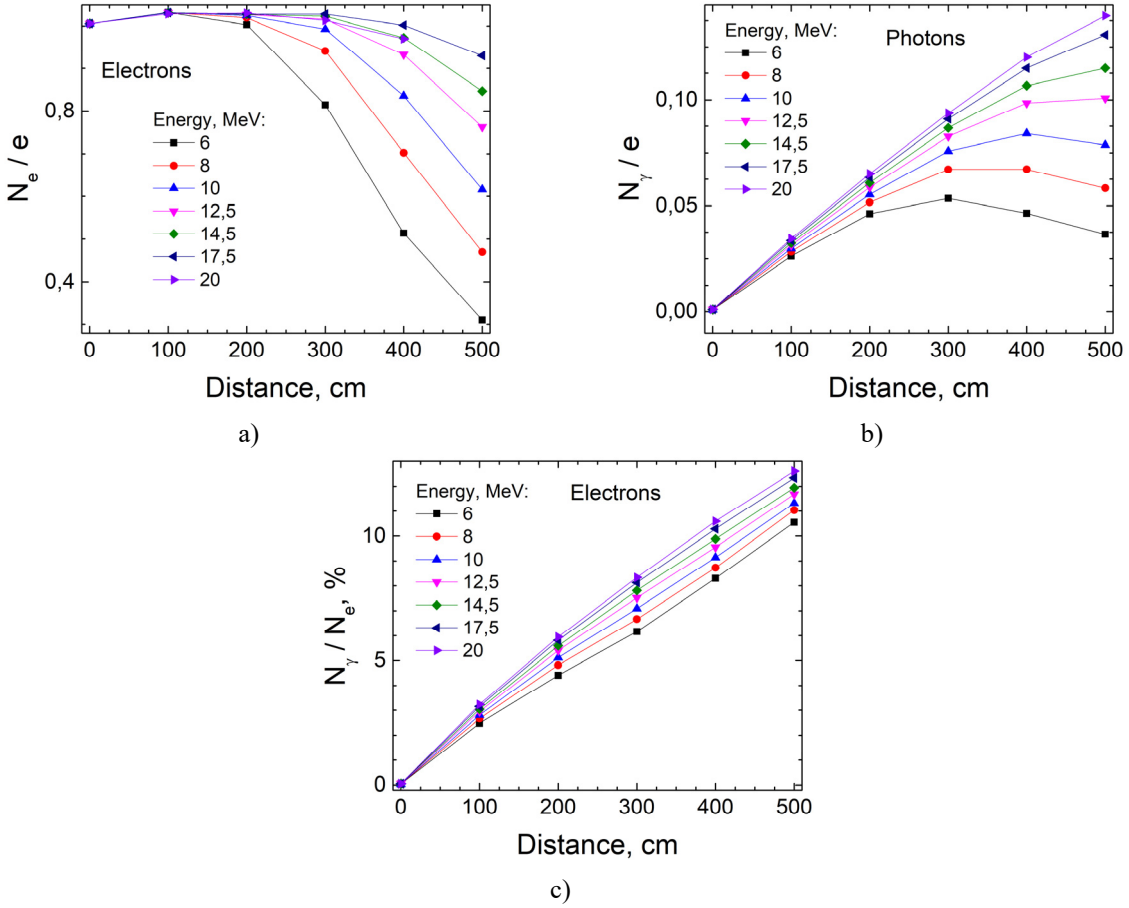

Figure 9. Dependence of the integral values of the quantities of electrons (a) and secondary photons (b), and the percentage of photons in the electron beam (c), on the distance at fixed values of the initial electron energy

Table 2. The dependence of integral quantitative values of electrons, secondary photons falling on the PPP, and the percentage of secondary photons in the electron beam on the initial electron energy at fixed distances

Distance, cm		**Initial electron energy, MeV**						
		6	**8**	**10**	**12.5**	**14.5**	**17.5**	**20**
0.1	N_e/e	1.006 0	1.0060	1.0060	1.0060	1.0060	1.0060	1.0060
	N_γ/e	8.117E-4	8.645E-4	8.908E-4	9.338E-4	9.373E-4	9.826E-4	0.0010
	C	**0.04 %**	**0.04 %**	**0.04 %**	**0.05%**	**0.05%**	**0.05%**	**0.05 %**
100	N_e/e	1.0326	1.0319	1.0319	1.0316	1.0317	1.0317	1.0318
	N_γ/e	0.0263	0.0283	0.0298	0.03133	0.0323	0.0336	0.0345
	C	**2.48 %**	**2.67 %**	**2.81 %**	**2.95 %**	**3.04 %**	**3.15 %**	**3.23 %**
200	N_e/e	1.0033	1.0199	1.0249	1.0270	1.0278	1.0287	1.0290
	N_γ/e	0.0462	0.05160	0.0553	0.0586	0.0608	0.0634	0.0651
	C	**4.41 %**	**4.82 %**	**5.12 %**	**5.40 %**	**5.59 %**	**5.81 %**	**5.95 %**
300	N_e/e	0.8147	0.9409	0.9930	1.0164	1.0235	1.0284	1.0306
	N_γ/e	0.0535	0.0672	0.0758	0.0827	0.0867	0.0910	0.0937
	C	**6.16 %**	**6.66 %**	**7.09 %**	**7.52 %**	**7.81 %**	**8.13 %**	**8.33 %**
400	N_e/e	0.5137	0.7025	0.8358	0.9321	0.9725	1.0023	1.0135
	N_γ/e	0.0465	0.0672	0.0841	0.0985	0.1067	0.1149	0.1200
	C	**8.30 %**	**8.73 %**	**9.15 %**	**9.56 %**	**9.88 %**	**10.29 %**	**10.59 %**
500	N_e/e	0.3099	0.4694	0.6158	0.7621	0.8469	0.9298	0.9699
	N_γ/e	0.0366	0.0582	0.0786	0.1008	0.1149	0.1308	0.1399
	C	**10.55 %**	**11.04 %**	**11.32 %**	**11.68 %**	**11.95 %**	**12.33 %**	**12.60 %**

The calculated dependences N_e/e, N_γ/e, and C are consistent with the results of similar studies for the same initial electron energies and distances to the irradiation objects [11,26,27].

The simulation results allowed us to obtain profiles of electron beams and generated secondary photons in the PPP with size 100×100 cm (for a distance of 100 cm from the accelerator output unit) at initial electron energies of 6, 12.5, and 20 MeV (Figure 10). A heat map of electron and secondary photon distribution probability was made based on the results achieved. It was found that an increase in the initial energy of electrons leads to a decrease in the angular distribution of particles (electrons, bremsstrahlung photons) and to an increase in their concentration in the center of the PPP.

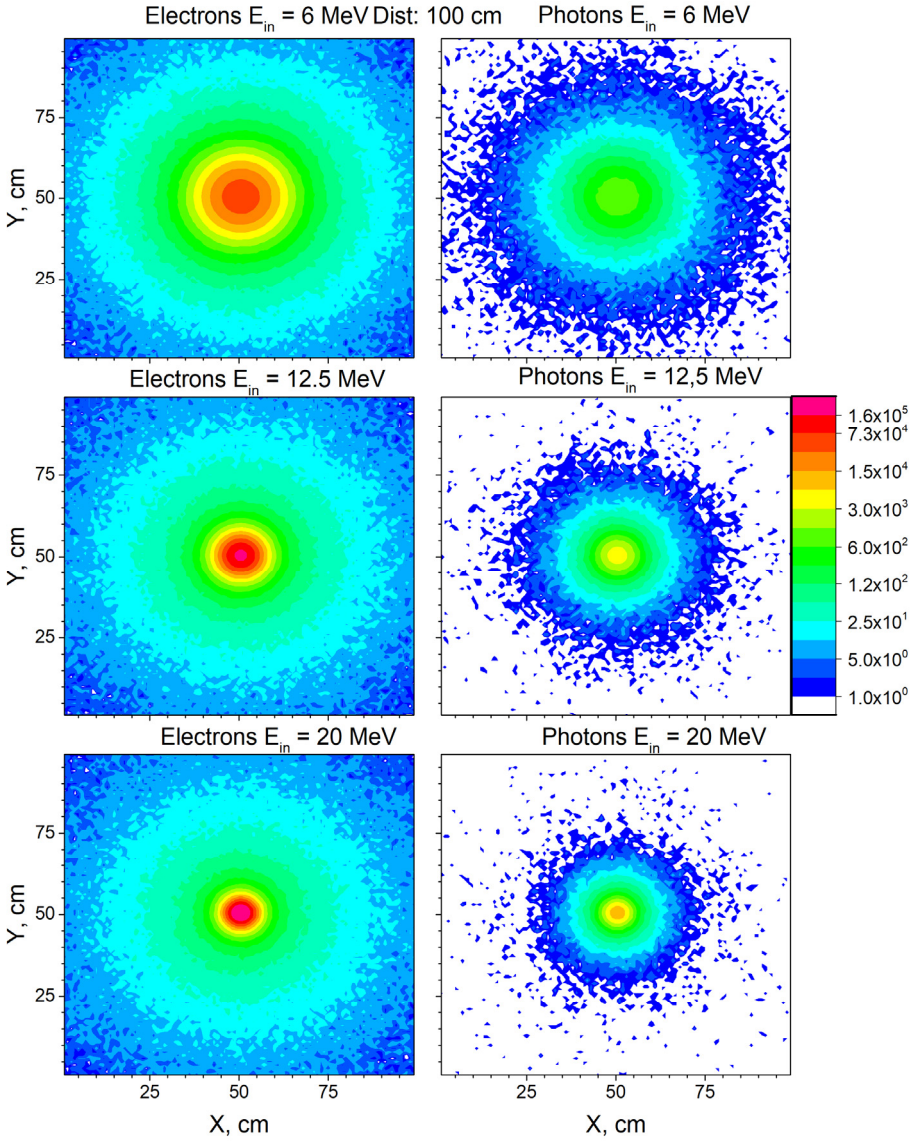

Figure 10. Profiles of electrons and secondary photons incident on a plane at fixed values of the initial electron energy

From the obtained profiles in the section on planes of size 100×100 cm (for a distance of 100 cm from the accelerator output unit) (Figure 10), transverse distributions of the intensity of electrons and secondary photons along the X axis perpendicular to the beam axis in the center of PPP (Figure 11) were taken. The cross-section graph confirms the conclusions mentioned above and clearly demonstrates the increase in particle concentration in the center of the irradiated plane. The numerical values of the calculated peak areas of the sections at the initial electron energies of 6, 12.5, and 20 MeV are 6.990×10^5, 1.381×10^6, 2.084×10^6 for electrons and 1.4469×10^4, 3.4537×10^4, 5.8380×10^4 for bremsstrahlung photons, respectively.

The obtained results reflect the general patterns of the influence of the initial energy of electron beams on their spatial distributions at fixed distances and the spatial distributions of secondary bremsstrahlung photons generated in air. The obtained results are consistent with similar studies [10,11,19,41].

Any differences between the investigated characteristics may be related to the technical parameters of the accelerators (electron ejection units). They can significantly affect the final characteristics of the electron beams and bremsstrahlung photon fluxes in the PPP of the samples [28,29].

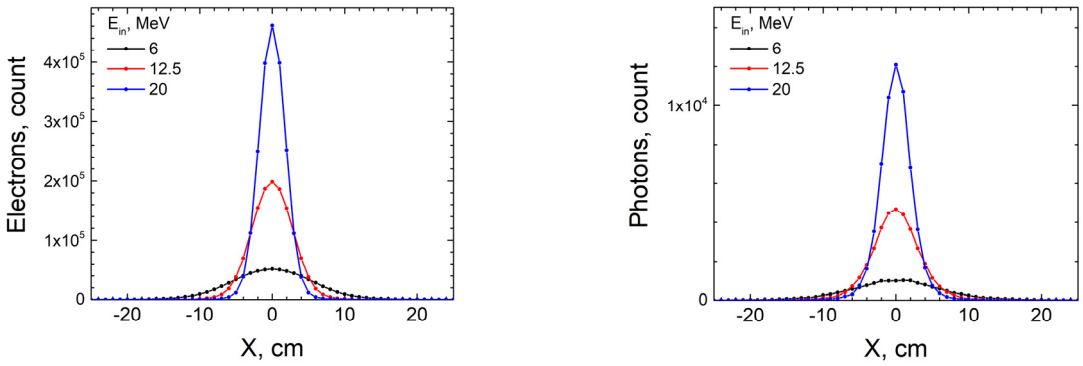

a) b)

Figure 11. Transverse distributions of the intensity of the electron beam (a) and the generated secondary photons (b) on the central X axis (0 – the center of the PPP of the sample) at the initial electron energies.

CONCLUSIONS

The results of modeling studies using the Monte Carlo code GEANT4 made it possible to establish the influence of air layers on the change in the initial characteristics of electron beams during their transportation to irradiation objects and on the parameters of the generated bremsstrahlung photon fluxes in the plane of placement of experimental samples.

The computer simulations of changes in the characteristics of electron beams and bremsstrahlung photon fluxes generated in the air layers between the M-30 microtron output unit and the plane of placement of experimental samples will allow finding optimal schemes for their radiation treatment, for example, obtaining uniform particle fields in the plane of their location, taking into account their geometric dimensions. In addition, the simulation results will allow for the prediction of effective and optimal practical applications to conduct a reliable assessment of the absorbed dose during interaction with electron beams and the contribution of additional dose from interaction with bremsstrahlung photon fluxes.

The proposed simulation scheme can be used to optimize the irradiation processes of experimental samples on different types of accelerators with various technical parameters.

This work was carried out within the framework of the topic “Excitation, ionization, luminescence of atomic and molecular systems under the action of photons and electrons,” State Registration No. – 0124U000782

ORCID IDs

Eugene V. Oleinikov, https://orcid.org/0000-0003-0949-5145; **Eugene Yu. Remeta,** https://orcid.org/0000-0001-9799-7895
Yurii Yu. Bilak, https://orcid.org/0000-0001-5989-1643; **Aleksandr I. Gomonai,** https://orcid.org/0000-0003-4341-699X
David Chvatil, https://orcid.org/0009-0007-1821-5850

REFERENCES

[1] F. Méot. Understanding the Physics of Particle Accelerators. A Guide to Beam Dynamics Simulations Using ZGOUBI // Springer Cham. 2024. 636 p. https://doi.org/10.1007/978-3-031-59979-8
[2] F. Frei, S. Vörös, M. Lüthi, P. Peier, Nuclear Instruments and Methods in Physics Research A, **1077**, 170588 (2025). https://doi.org/10.1016/j.nima.2025.170588
[3] A. Ikhlaq, S.A. Buzdar, M. Aslam, M.U. Mustafa, S. Salahuddin, M. Nisa, Scientific Inquiry and Review, **5**(3), 13 (2021). https://doi.org/10.32350/sir/52
[4] S.D. Quoc, T. Fujibuchi, H. Arakawa, K. Hamada, D.H. Han, Applied Radiation and Isotopes, **219**, 111704 (2025). https://doi.org/10.1016/j.apradiso.2025.111704
[5] Md.K. Hasan, D. Staack, S.D. Pillai, L.S. Fifield, M. Pharr, Polymer Degradation and Stability, **221**, 110677 (2024). https://doi.org/10.1016/j.polymdegradstab.2024.110677
[6] Z. Chu, H. Wang, B. Dong, Molecules, **29**(14), 3318 (2024). https://doi.org/10.3390/molecules29143318
[7] A.G. Chmielewski, Radiation Physics and Chemistry, **213**, 111233 (2023). https://doi.org/10.1016/j.radphyschem.2023.111233
[8] Y. Wang, D. Chen, R.S. Augusto, J. Liang, Z. Qin, J. Liu, Z. Liu, Molecules, **27**(16), 5294 (2022). https://doi.org/10.3390/molecules27165294
[9] J. Bendahan, Nuclear Instruments and Methods in Physics Research Section A, **954**. 161120 (2020). https://doi.org/10.1016/j.nima.2018.08.079
[10] A. Ryczkowski, T. Piotrowski, M. Staszczak, M. Wiktorowicz, P. Adrich, Zeitschrift für Medizinische Physik, **34**(4), 510 (2024). https://doi.org/10.1016/j.zemedi.2023.03.003
[11] C. Oproiu, M.R. Nemţanu, M. Braşoveanu, and M. Oane, “Determination of absorbed dose distribution in technological accelerated electron beam treatments,” in: *Practical Aspects and Applications of Electron Beam Irradiation*, ch. 2, edited by M.R. Nemtanu and M. Brasoveanu (Transworld Research Network, 2011). p. 17-41.
[12] W. Strydom, W. Parker, and M. Olivares, “Electron beams: Physical and clinical aspects,” in: *Review of Radiation Oncology Physics: A Handbook for Teachers and Students*, Chapter 8, tech. editor E.B. Podgorsak, International Atomic Energy Agency Library Cataloguing in Publication Data. Vienna: 2005. p. 273-300. https://www-pub.iaea.org/MTCD/publications/PDF/Pub1196_web.pdf
[13] H.O. Tekin, T. Manici, E.E. Altunsoy, K. Yilancioglu, and B. Yilmaz, Acta Physica Polonica A, **132**(3-II), 967 (2017). https://doi.org/10.12693/APhysPolA.132.967
[14] M.K. Saadi, and R. Machrafi, Applied Radiation and Isotopes, **161**, 109145 (2020). https://doi.org/10.1016/j.apradiso.2020.109145

[15] G.X. Ding, S. Kucuker-Dogan, and I.J. Das, Medical Physics, **49**(2), 1297 (2022). https://doi.org/10.1002/mp.15433
[16] V.A. Shevchenko, A.Eh. Tenishev, V.L. Uvarov, and A.A. Zakharchenko, Problems of Atomic Science and Technology, (6), 163 (2019). https://doi.org/10.46813/2019-124-163
[17] V.L. Uvarov, A.A. Zakharchenko, L.V. Zarochintsev, *et al*., Problems of Atomic Science and Technology, (3), 154 (2020). https://doi.org/10.46813/2020-127-154
[18] M.R.M. Chulan, M.F.M. Zin, L.K. Wah, M. Mokhtar, M.A. Ahmad, A.H. Baijan, R.M. Sabri, and K.A. Malik, IOP Conf. Series: Materials Science and Engineering, **785**, 012003 (2020). https://doi.org/10.1088/1757-899X/785/1/012003
[19] P. Apiwattanakul, and S. Rimjaem, Nuclear Inst. and Methods in Physics Research B, **466**, 69 (2020). https://doi.org/10.1016/j.nimb.2020.01.012
[20] R.I. Pomatsalyuk, V.A. Shevchenko, D.V. Titov, A.Eh. Tenishev, V.L. Uvarov, A.A. Zakharchenko, and V.N. Vereshchaka, Problems of Atomic Science and Technology, (6), 201 (2021). https://doi.org/10.46813/2021-136-201
[21] H. Kim, D.H. Jeong, S.K. Kang, M. Lee, H. Lim, S.J. Lee, and K.W. Jang, Nuclear Engineering and Technology, **55**, 3417 (2023). https://doi.org/10.1016/j.net.2023.05.033
[22] A. Toutaoui, A.N. Aichouche, K. Adjidir, and A.C. Chami, Journal of Medical Physics, **33**, 141 (2008). https://doi.org/10.4103/0971-6203.44473
[23] G.X. Ding, Z.(J) Chen, and K. Homann, Medical Physics, **51**, 5563 (2024). https://doi.org/10.1002/mp.17186
[24] J. Tertel, J. Wulff, H. Karle, and K. Zink, Zeitschrift für Medizinische Physik, **30**(10), 51 (2010). https://doi.org/10.1016/j.zemedi.2009.11.001
[25] M.R.S. Didi, M. Zerfaoui, M. Hamal, Y. Oulhouq, and A. Moussa, Radiation Physics and Chemistry, **207**, 110859 (2023). https://doi.org/10.1016/j.radphyschem.2023.110859
[26] G.X. Ding, S. Kucuker-Dogan, and I.J. Das, Medical Physics, **49**(2), 1297 (2022). https://doi.org/10.1002/mp.15433
[27] N. Khaledi, D. Sardari, M. Mohammadi, A. Ameri, and N. Reynaert, Journal of Radiotherapy in Practice, **17**, 319 (2018). https://doi.org/10.1017/S1460396917000711
[28] A. Ryczkowski, T. Piotrowski, M. Staszczak, M. Wiktorowicz, and P. Adrich, Zeitschrift für Medizinische Physik, **34**(4), 210 (2024). https://doi.org/10.1016/j.zemedi.2023.03.003
[29] A. Ryczkowski, B. Pawałowski, M. Kruszyna-Mochalska, A. Misiarz, A. Lenartowicz-Gasik, M. Wosicki, A. Jodda, *et al*., Polish Journal of Medical Physics and Engineering, **30**, 177 (2024). https://doi.org/10.2478/pjmpe-2024-0021
[30] V.T. Maslyuk, Visnyk of the National Academy of Sciences of Ukraine, **11**, 46 (2016). https://doi.org/10.15407/visn2016.11.046
[31] Professional public organization «Ukrainian Association of Medical Physicists», Remote radiation therapy in Ukraine. https://uamp.org.ua/useful-information/radiotherapy-equipment-in-ukraine/external-radiotherapy/ (in Ukrainian)
[32] GEANT4 11.1 (9 December 2022). https://geant4.web.cern.ch/download/11.1.0.html
[33] S. Ashurov, S. Palvanov, A. Tuymuradov, and D. Tuymurodov, Bulletin of National University of Uzbekistan Mathematics and Natural Sciences, **6**(4), 179 (2023). https://doi.org/10.56017/2181-1318.1257
[34] T.V. Malykhinaa, V.E. Kovtuna, V.I. Kasilovb, and S.P. Gokov, East European Journal of Physics, **4**, 91 (2021). https://doi.org/10.26565/2312-4334-2021-4-10
[35] E. Oleinikov, I. Pylypchynets, and O. Parlag, Journal of Nuclear and Particle Physics, **13**, 7 (2023). https://doi.org/10.5923/j.jnpp.20231301.02
[36] E.V. Oleinikov, I.V. Pylypchynets, O.O. Parlag, and V.V. Pyskach, **153**(5), 148 (2024). https://doi.org/10.46813/2024-153-148
[37] OriginLab Corporation, One Roundhouse Plaza, Suite 303, Northampton, MA 01060, UNITED STATES, OriginPro, https://www.originlab.com/
[38] R. Maskani, M.J. Tahmasebibirgani, M.H. Ghahfarokhi, and J. Fatahias, Asian Pacific Journal of Cancer Prevention, **16**(17), 7795 (2015). https://doi.org/10.7314/APJCP.2015.16.17.7795
[39] M. Rezzoug, M. Zerfaoui, Y. Oulhouq, and A. Rrhioua, Reports of Practical Oncology & Radiotherapy, **28**(5), 592 (2023). https://doi.org/10.5603/rpor.96865
[40] M. Rezzoug, M. Zerfaoui, Y. Oulhouq, A. Rrhioua, S. Didi, M. Hamal, and A. Moussa, Radiation Physics and Chemistry, **207,** 110859 (2023). https://doi.org/10.1016/j.radphyschem.2023.110859
[41] M.A. Pagnan-González, J.O. Hernández-Oviedo, and E. Mitsoura, Revista de Medicina e Investigación, **3**(1), 22 (2015). https://doi.org/10.1016/j.mei.2015.02.002

МОДЕЛЮВАННЯ ХАРАКТЕРИСТИК ПУЧКІВ ЕЛЕКТРОНІВ ТА ЗГЕНЕРОВАНИХ ПОТОКІВ ФОТОНІВ НА МІКРОТРОНІ М-30

Євген В. Олейніков[a], Давід Хватіл[b], Євген Ю. Ремета[a], Олександр І. Гомонай[a], Юрій Ю. Білак[c]
[a]Інститут електронної фізики НАН України, Ужгород, Україна
[b]Інститут ядерної фізики Чеської Академії Наук, Чеська республіка
[c]ДВНЗ «Ужгородський національний університет», Ужгород, Україна

Забезпечення оптимізації процесу радіаційної обробки експериментальних зразків на електронних прискорювачах та ефективне прогнозування результатів взаємодії пучків електронів з об'єктами опромінення потребують максимально точної інформації про характеристики пучків. Початкові (первинні) характеристики пучків електронів прискорювачів при транспортуванні до об'єктів опромінювання будуть змінюватися внаслідок їх взаємодії з зовнішнім середовищем (повітрям). Так, додатково відбувається генерація вторинних частинок – гальмівних фотонів, які теж взаємодіють зі зразками. У роботі представлені результати досліджень з моделювання впливу шарів повітря на зміну початкових характеристик пучків електронів при їх транспортуванні до об'єктів опромінення та на параметри згенерованих потоків гальмівних фотонів у площині розміщення експериментальних зразків. У дослідженнях використовувався Монте-Карло код – GEANT4. Моделювання проводилося на прикладі електронного прискорювача ІЕФ НАН України – мікротрону М-30 з врахуванням його технічних параметрів. Представлено результати досліджень характеристик (енергетичні спектри, їх інтегральні значення, поперечні розподіли у площині 10×10 см) пучка електронів і вторинних фотонів на виході електронного прискорювача. Вивчено вплив товщин шарів повітря (0.1÷500 см) між блоком виводу електронів та потенційною площиною (100×100 см) розміщення експериментальних зразків для опромінення на характеристики первинних пучків електронів та згенерованих гальмівних фотонів (для області енергій 6÷20 МеВ).

Ключові слова: *мікротрон; GEANT4; пучок електронів; гальмівне випромінювання; Ті віконце; повітря; спектр; просторовий розподіл*